

Synthesis and Characterization of Nanoporous Silver Foams

Dana Hess

Department of Chemistry & Physics
California University of Pennsylvania
250 University Avenue
California, PA 15419 USA

Faculty Advisor: Kimberly Woznack

Abstract

Synthesis of nanoporous silver foam was accomplished using H₂ coevolution method, a method that has been successfully employed by researchers to synthesize metallic foams of Cu, Ni and Sn. This procedure was carried out in a solution of HNO₃ and AgNO₃. After repeating this synthesis in varying potentials and concentrations of H⁺ and Ag⁺, characterization of the foam was carried out by scanning electron microscope (SEM), powder x-ray diffraction (XRD) and energy dispersive spectrometry (EDS). EDS confirmed the foam was silver by a sharp peak at the silver n=3 to 2 (L_{α1}) transition value of 2.983 keV. Powder XRD confirmed a silver material with a crystal structure of Fm3m, a=4.0861, α=90.0000. SEM analysis showed the presence of silver nanoparticles attached to large dendrite structures. Silver ion concentration and voltage showed direct relationships to dendrite surface imperfections and nanoparticle concentrations, while hydrogen ion concentration showed an inverse relationship.

Keywords: Electrodeposition, Batteries, Nanoparticles

1. Background

Prized for their low mass, good electrical conductance, impact absorbance and high surface area to volume ratio, nanoporous metallic foams are finding uses in many industries. Materials showing a high surface area and good electrical conductance, such as nanoporous foams, could be used to build a new type of galvanic cell with an increased velocity of charge transfer. Such materials are being explored now, and have the possibility to drastically increase the energy density of existing types of batteries while significantly decreasing the time required to recharge. For this experiment, nanoporous silver will be electrodeposited in acidic solution, and its properties will be characterized.

The physical characteristics of a nanoporous foam depend on the conditions present during the synthetic process.^{1,2} Varying the conditions of the synthetic process can enhance different characteristics of the foam. For this experiment, silver was chosen specifically due to its high conductivity in both elemental and salt compounds. Previous work has shown a successful application of the Hydrogen (H₂) Co-evolution method to synthesize nanoporous foams of nickel, tin and copper.³ The goal of this investigation was to utilize and optimize this method for the synthesis of nanoporous silver foam.

Electrodeposition of silver is non-spontaneous; therefore, some amount of electric potential must be applied for deposition and overcoming solution resistivity (overpotential).⁴ The standard reduction potential of Ag⁺ to Ag_(s) is

$Ag_{(aq)}^+ + e^- \rightarrow Ag_{(s)}$, $E^0 = 0.7993V$.⁴ For an electrolytic deposition, a sufficient potential must be applied to bring about a reduction of the desired species. As H⁺ reduction's potential is lower in magnitude than Ag⁺, a potential that is low enough to reduce H⁺ will also cause reduction of Ag⁺. This minimum value can be calculated using the Nernst Equation, shown in equation 1:⁴

$$E_{cell} = E_{Ag} + E_{H_2} = 0.7993V - 0.0592 \log \frac{1}{[Ag^+]} - \frac{0.0592}{2} \log \frac{1}{[H^+]^2} \quad (1)$$

The H_{2(g)} Co-evolution Method applies a significant negative overpotential to the solution, creating an environment in which a linear electrodeposition is unfavored.³ During electrolysis, H_{2(g)} bubbles are generated on the surface of the cathode, and this evolution was used as a negative electro-depositional space for the reducing metal. In Cu, Ni and Sn, this process yielded light, open-celled structures with a high surface area. For Ag, this procedure was carried out in a solution of HNO₃ and AgNO₃. To compare foam size and uniformity, this synthesis was repeated in varying voltages and concentrations of H₃O⁺ and Ag.

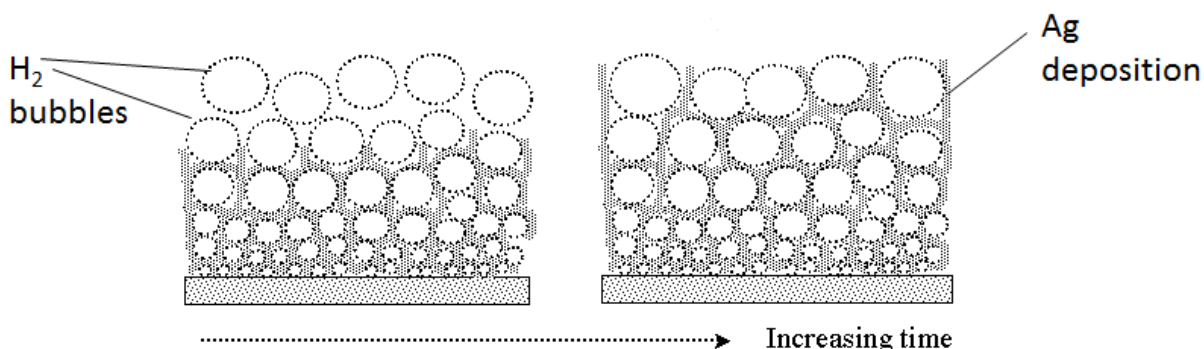


Figure 1. A pictorial representation of the H₂ Co-evolution Method. Gaseous hydrogen forms a non-spontaneous depositional space, forcing silver deposition outside of the bubbles.³

Because galvanic and electrochemical reactions require a charge transfer involving at least one solid component, surface area plays an important role in the speed of reaction. Anions and cations must negotiate the repulsive effects of nearby similarly charged ions to interact with the contact surface and make an electron transfer. In fact, surface area is the primary physical inhibitor, and it is directly related to the velocity of charge transfer. Most existing technology, such as commercial batteries, use materials that essentially allow charge transfer in two dimensions. Addition of a third dimension to the contact allows for a large increase in substrate interaction area. Nanoporous materials exhibit this characteristic, with surface areas that range from 500 to 7500 m²/m³.¹ There has been substantial research into the role of three-dimensional contacts in galvanic cells, and that research suggests a significant increase in the velocity of charge transfer, both in discharging and charging the cell.⁵

2. Methods

2.1 Preparation of Stock Solutions

Concentrated HNO₃ (15.7M, 63.943mL, CAS# 7697-37-2) was added to a 500.00 mL volumetric flask using two Fisher Finnpipettes (2 to 10mL ±60.0 μL; 2 to 200μL ±4.0 μL)⁶. The volumetric flask was then filled to the line with deionized water, giving a stock solution with a pH of -0.3027. A 1.00M solution of AgNO₃ was made by first weighing out 84.9347g of AgNO₃ (CAS# 7761-88-8) with a Mettler AE 100 Analytical Balance (±0.0001 g).

2.2 Cathode Construction

Foam synthesis was accomplished using the H₂ coevolution method. A silver cathode contact was made using approximately 4cm of platinum wire with a coil of approximately 0.75cm diameter at the end. This coil was bent orthogonal to the wire in two dimensions. The length of the wire was then slid into a thin glass Pasteur pipet and placed over a Bunsen burner to shrink wrap the wire. A piece of silver foil (CAS #7440-22-4, Lot MKDK2394V) was bent over the Pt coil with pliers, providing approximately 0.75cm² for electrodeposition. Care was taken to crimp the edges of the silver together, to minimize interaction between the aqueous silver and the wire. The wire was connected to the anode of a B&K Model 1601 Regulated DC Power Supply (±0.05 V).

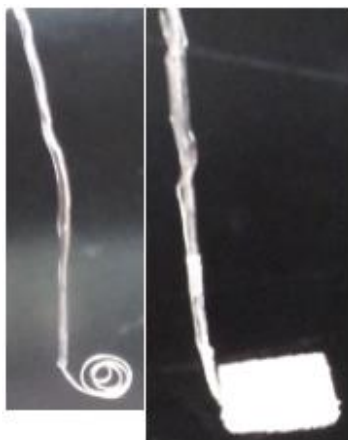


Figure 2. Examples of the silver cathode, with silver foil contact (right)

2.3 Synthesis Of Silver Nanoporous Foam

The cathode was submerged in a solution of AgNO_3 and HNO_3 . Exact concentrations were varied and recorded as shown in Table 1. A small piece of bare Pt wire was allowed to touch the surface of the solution, dipping in a few millimeters. A nine- inch Pasteur pipet, connected by rubber hosing to a smaller Pasteur pipet seated in a rubber stopper, was submerged as deep as possible, with the small opening of the pipet below the Ag contact. The rubber stopper was placed in the top opening of a side arm flask, with rubber tubing connected to the side arm going to an aspirator pump. A potential was applied to the cathode, and this voltage was maintained throughout the reaction. Voltages were varied and recorded. Once the reaction reached equilibrium (the solution turned from transparent brown back to clear), the voltage was removed and the vacuum pump was maintained at a low rate. Deionized water was used to replace the reaction solution. This was done by spraying a small amount at a time against the side of the test tube, just above the liquid line, and allowing it to flow down into the solution with minimal mixing.

Table 1. Concentration, voltage and amperes for each synthesis.

Trial	[Ag⁺]	[H₃O⁺]	Volts (V)	Amperes (A)
1	0.40M	1.00M	3.0	0.50
2	0.40M	1.00M	4.0	0.30
3	0.40M	0.50M	3.0	0.06
4	0.50M	0.50M	3.0	0.06
5	0.50M	0.50M	3.0	0.06
6	1.00M	0.50M	3.0	0.06
7	0.75M	0.50M	3.0	0.06
8	0.60M	0.50M	3.0	0.06
9	0.50M	0.50M	3.0	0.60
10	0.20M	0.50M	3.0	0.60
11	0.40M	0.50M	2.0	0.30
12	0.40M	0.50M	3.5	0.40
13	0.60M	0.50M	4.0	0.40
14	0.50M	0.50M	4.0	0.40
15	0.50M	0.50M	4.0	0.40
16	0.40M	0.50M	4.0	0.40
17	0.20M	0.50M	4.0	0.40

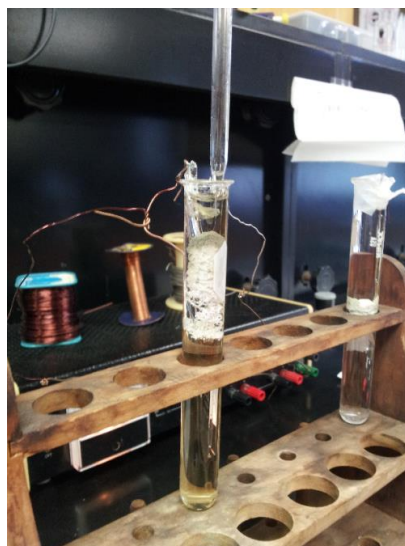


Figure 3. A photo of the reaction vessel. Cathode (left wire) has an example of the nanoporous foam, *in situ*.

3. Results

3.1 Electrodeposition

Deposition resulted in a composite structure, with a larger, sturdier dendrite formation supporting a soft, slushy foam (Figure 4). During deposition, the anode was observed to produce a dark green to black precipitate and gas bubbles. This precipitate would further react by producing gas bubbles, and it disappeared before or soon after reaching the bottom of the vessel. Sample solution was drained, and the sample was separated from the contact for further analysis.

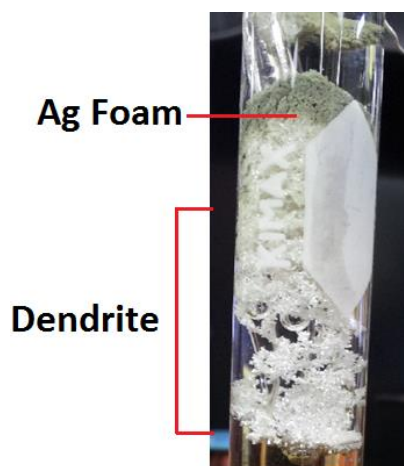


Figure 4. A macroscopic view of the foam and dendrites

3.2 Energy Dispersive Spectroscopy (EDS)

EDS analysis was carried out on Trial 13, using a Bruker Quantax with Xflash 5010. An electric current was sent into the sample to excite electrons, and an x-ray emission was observed from the resulting electron relaxation. The emitted x-ray light was found to be 2.983keV, which matched the $n=3$ to 2 ($L_{\alpha 1}$) transition value of silver (Figure 5).

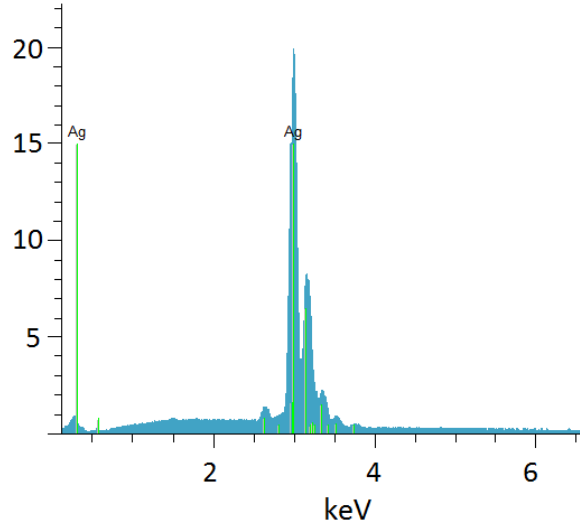


Figure 5. EDS measurement of emitted X-ray from Trial 13.

3.3 Powder X-ray Diffraction (XRD)

Powder XRD was accomplished using a PANalytical X'Pert PRO powder x-ray diffractometer. Four of the trials were scanned on one hour scans, 5-80° 2θ (Table 1). All samples showed a pure silver material, with a crystal structure corresponding to $Fm\bar{3}m$, $a=4.0861$, $\alpha=90.0000$.²³ Figure 6 shows the XRD peaks, normalized, for each sampled trial. Peak broadening, indicative of nanoparticles, was not observed.

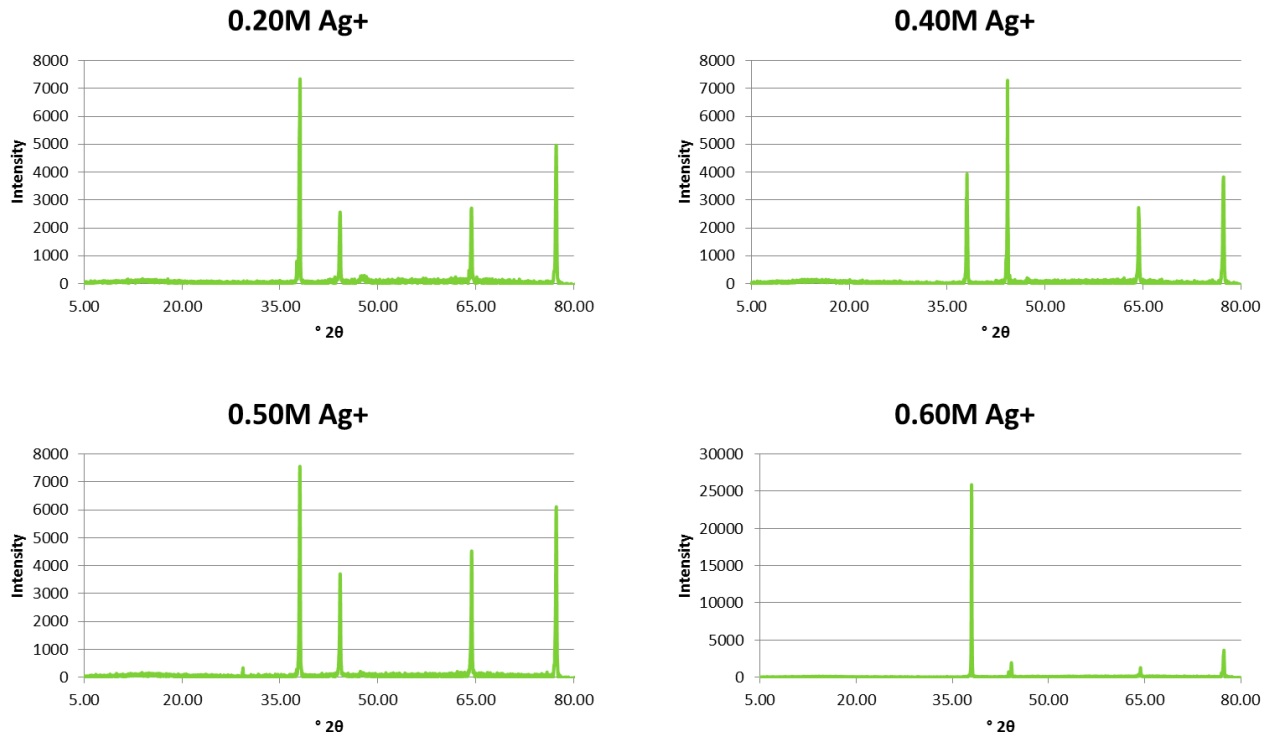


Figure 6. XRD analyses for Trials 10, 12, 13 and 14.

3.4 Scanning Electron Microscopy (SEM)

SEM analysis was done using a Hitachi S3400N SEM. Samples were scanned for particle size (Table 1). Examples of dendrite and foam (left and right columns, respectively) synthesized are pictured in Figures 7-10.

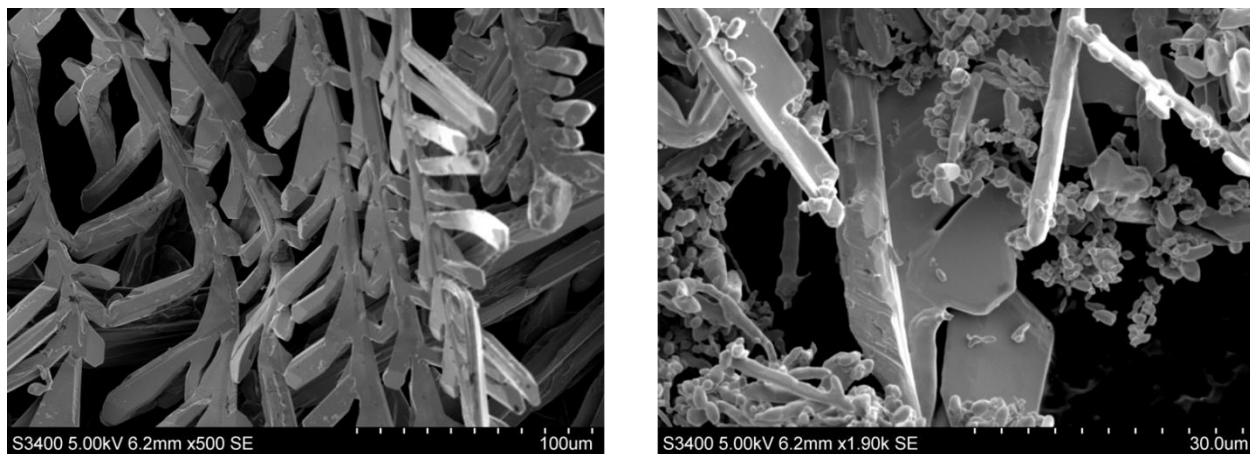


Figure 7. Dendrite and nanoparticles, 0.20 M Ag^+ (Trial 10)

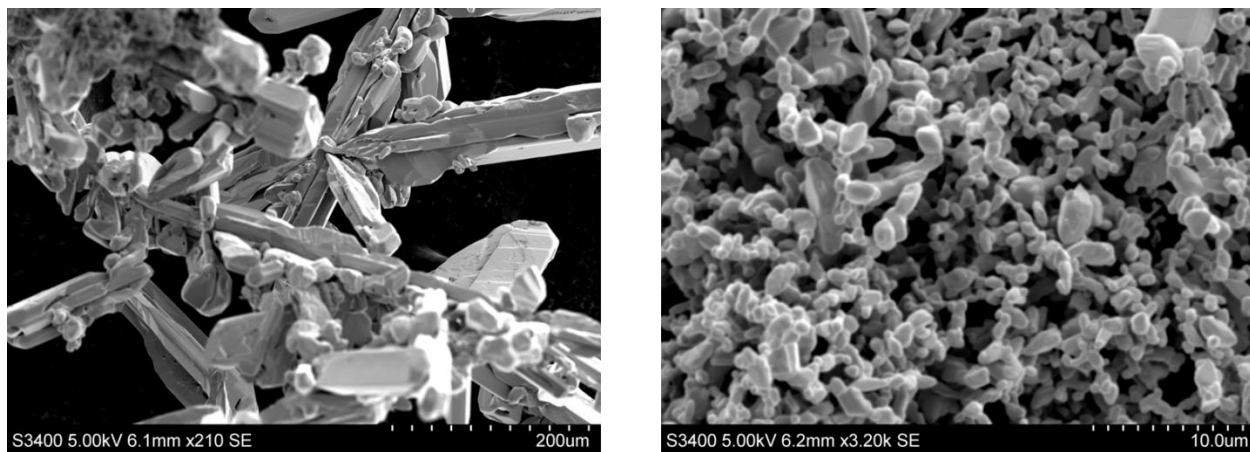


Figure 8. Dendrite and nanoparticles, 0.40 M Ag^+ (Trial 12)

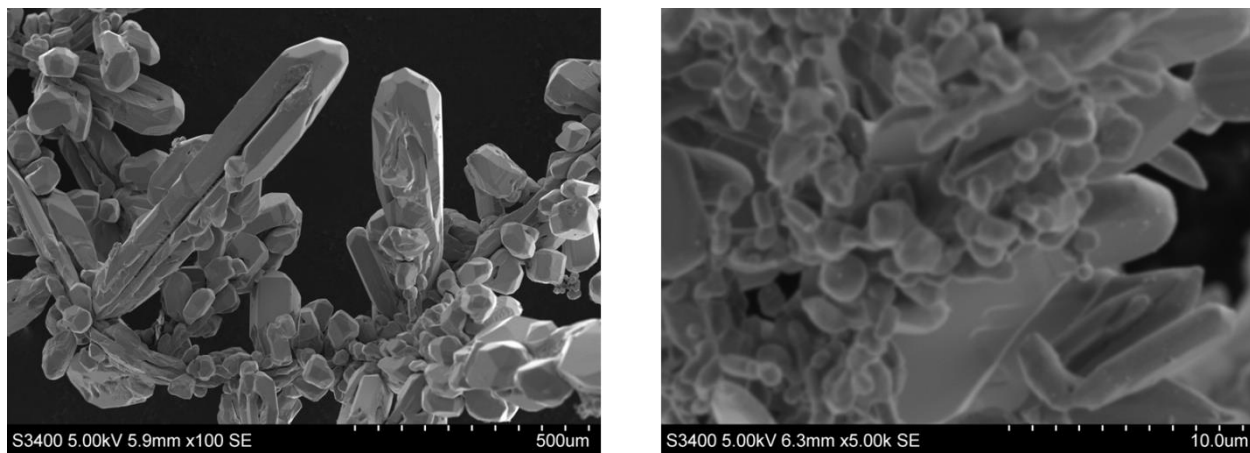


Figure 9. Dendrite and nanoparticles, 0.50 M Ag^+ (Trial 14)

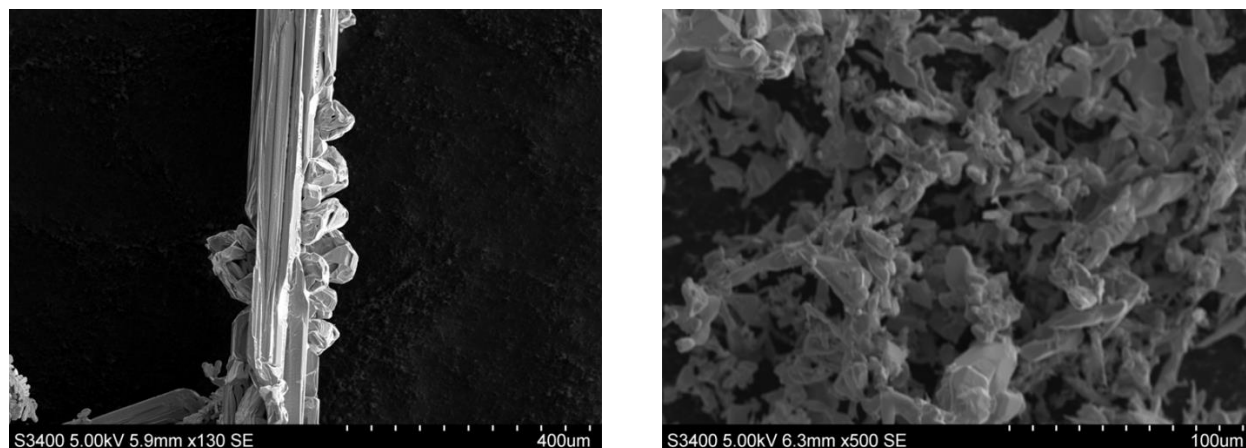


Figure 10. Dendrite and nanoparticles, 0.60 M Ag⁺ (Trial 13)

EDS and XRD validated the H₂ coevolution method produced a pure silver structure (Figure 5.). Literature shows a value of 2.98460 keV for an n=3 to 2 transition for silver (L_{α1}).²⁴ An experimentally found value of 2.983 keV was a match to this, with a percent error of 0.03351%. XRD analysis showed the best match for each sample was the silver crystal structure Fm3̄m, a=4.0861, α=90.0000. EDS and XRD confirm the samples are composed of a pure silver crystal structure.²³ Some degradation due to oxidation could be seen in the final XRD analysis run, 0.60 M (Figure 6).

4. Discussion

The four trials analyzed, Trials 10, 12, 13 and 14, contain four different initial silver ion concentrations: 0.20, 0.40, 0.60 and 0.50 mol/L, respectively. Potential for these trials were 3.0, 3.5 and 4.0 volts (Trials 13 and 14). It was at these potentials that H_{2(g)} reduction began to occur. This voltage increased with concentration of Ag⁺ as predicted; however, the potential necessary to cause hydrogen and silver ion reduction simultaneously was considerably higher than that predicted by the Nernst Equation (Table 2). For Trial 10, for instance, this calculation would be:

$$E_{cell} = 0.7993V - \frac{0.0592}{1} \log\left(\frac{1}{0.20M}\right) + 0.000 - \frac{0.0592}{2} \log\left(\frac{1}{(0.50M)^2}\right) = 3.0V \quad (2)$$

Table 2. Concentrations of silver and hydrogen ions and predicted potentials in analyzed trials.

	[Ag ⁺] (mol/L)	[H ⁺] (mol/L)	E _{cell} Predicted (volts)	E _{cell} Observed (volts)
Trial 10	0.20	0.50	0.74	3.0
Trial 12	0.40	0.50	0.76	3.5
Trial 13	0.60	0.50	0.77	4.0
Trial 14	0.50	0.50	0.76	4.0

This voltage gap would require large concentrations of interfering ions. As EDS and XRD show a pure silver compound, the only ions introduced in solution are Ag^+ , NO_3^- and H^+ . A black precipitate was observed forming at the anode during synthesis. This must be silver ions interacting with oxygen, forming a dark green to black precipitate. As silver oxide left the anode and sunk to the bottom of the vessel, this reaction reverses; Ag_2O is attacked by the hydrogen ions, redissolving the ion. This is due to the hydrogen ion concentration: near the positively charged anode, hydrogen ions are repelled. This leads to a lower local concentration of H^+ . As the silver oxides leave this area, hydrogen ion concentration dramatically increases. Silver (II) oxide is vulnerable to attack by these hydrogen ions, and so AgO surrenders its oxygen ion readily.

If silver oxides are present, then some amount of oxygen must also be present in the area. Some of the water present in the area of the anode is being oxidized, releasing oxygen gas and hydrogen ions:¹



Some amount of these oxygen molecules escape the solution as gas, while some of them interact with the aqueous silver to form oxides.

In electrogravimetric analysis, nitrate ion (NO_3^-) is often used as a depolarizer.¹ This ion interacts with hydrogen ions at the cathode to form ammonium and water:^{1,25}



Ammonium ion is then able to make its way to the anode and be further oxidized to nitrogen gas:¹



The overall equation of this solution would be:

$$E_{\text{cell}} = E_{\text{Ag}^+} + E_{\text{H}^+} + E_{\text{NO}_3^-} - E_{\text{NH}_4^+} - E_{\text{HN}_3} - E_{\text{O}_2} \quad (7)$$

Hydrogen gas production, as with any electrochemical gas production, is highly unfavored. Without the use of a catalyst such as platinum, gases require a great deal of potential to produce. While a platinum wire was used, this wire was coated in a glass insulator and covered with a silver contact plate. Thus, some additional potential was necessary to produce hydrogen gas directly at the silver contact surface.

The overall effect of the silver concentration was directly related to the size, magnitude and entropy of both dendrite and nanoparticle formation. Increased concentration showed an increase in the thickness of dendrites formation, as well as augmented surface imperfections. By 0.60 mol/L, structures began to show pores (Figure 10) as well as the striations observed previously (Figures 8, 9). Uniformity in the dendrites broke down as well, as concentrations above 0.20 mol/L showed increasingly random appearances of branches (Figures 8, 9, 10). In low concentrations, structures showed a great deal of similarity in size, shape and direction of branch formations, and thickness. These concentrations also showed, predictably, a greater magnitude of dendrites, due to the larger amount of silver ions available in the solutions. Nanoparticles showed a similar response, with more variation in size and more aggregation in the higher concentration solutions.

Concentration of acid in the solution was not as large a factor as potential or silver concentration; however, its contribution cannot be ignored. Under natural conditions, nitric acid aggressively attacks pure silver and its oxides, releasing silver ions into solution. This factor was beneficial to creating a pure silver structure: any oxygen ions in solution were quickly converted to water. This also meant that the structure was being oxidized and destroyed by the acid as it was being reduced and formed, so it was imperative to remove the reaction solution as soon as synthesis was complete. A certain amount of free H⁺ ions were also necessary to provide a source of hydrogen gas. A concentration of 0.50 mol/L was found to provide the best balance of these three factors; hydrogen ions were available for H_{2(g)} generation, oxides were kept away from the sample and the silver structure was able to grow uninhibited.

The overall shape and structure of the samples was found to be less like a nanoporous foam and more like the dendritic silver structures produced by simple oxidation-reduction reactions with zinc or copper.^{26,27} However, by inducing an electric field by electrochemical reaction, this growth is focused into a specific direction. This process could be further refined by the use of an insulating material with sufficient resistance to nitric acid, such as glass. In low concentrations, structures showed a great deal of similarity in size, shape and direction of branch formations, and thickness (Figure 7).

At high concentrations, dendrites formed have a greater degree of dissimilarity. Similarly, nanoparticles forming in higher concentration solutions have a greater variability in size. This is due to availability of silver ion localized to the structure. In higher concentrations, silver ions experience more repulsion, and so are forced to be spread more densely. An induced electric field can then deposit more ions before kinetic polarization makes dendrite formation less favored.

More potential is necessary to make the hydrogen gas spontaneous as concentration of silver ion rises. This is also due to the availability of silver ions in solution. Applying the Nernst Equation to Ag⁺ at different concentrations (0.20 M and 0.40 M), the effect of concentration on initial deposition potential is apparent:

$$E_{cell} = 0.7993V - 0.0592 \log\left(\frac{1}{0.20M}\right) = 0.7579V \quad (8)$$

$$E_{cell} = 0.7993V - 0.0592 \log\left(\frac{1}{0.40M}\right) = 0.7757V \quad (9)$$

Increasing silver ion concentration increases the initial deposition potential. This shift seems to cause a change to the initial deposition potential of hydrogen ions in solution. As hydrogen ions are approximately six times as mobile as Ag⁺, mobility of hydrogen ions must be inhibited by the increased concentration of silver ions.

In solutions of 0.50 mol/L and higher, deep grooves and pores were observed in dendrite formations. These solutions required more time to complete deposition, and were therefore exposed to nitric acid in the reaction solution for a longer period of time. Aggressive attack by nitric acid on the structure is the most likely cause of these imperfections.

5. Conclusion

Use of nitric acid in electrochemical silver nanodeposition shows how very complex a solution can become with just a few variables. Aqueous ions of H⁺, NO₃⁻ and Ag⁺ quickly become more nuanced with the induction of an electric field, and variation in that field allowed for some control of the final deposition. Acid concentration, while less sensitive than potential and silver ion concentration, shows an inverse relationship, as excess acid aggressively attacks the deposited silver. This can account for some of the non-uniformity in structure.

While a true nanoporous compound was not synthesized, aqueous silver concentration did show a direct relationship to the entropy of the resulting structure. As aqueous silver increased in concentration, aggregation of silver nanoparticles at the outer Helmholtz layer also increased. These solid Ag particles, now removed from the solvated state, fell to the cathode and began to fuse, under their own weight, into dendrites. The resulting dendrites grew thicker and with less uniformity, likely due to overabundance of metal ions at favored binding sites.

Voltage showed a direct relationship with the size, magnitude and entropy of the silver dendrites. Increasingly negative potential leads to thicker dendrites, larger nanoparticles, and a more disordered structure. A greater negative potential has a greater attraction to the positive silver ions, and induces a crowded environment around the binding sites. While additional experimentation into this variable would better define this effect, it should hold true in any concentration.

Acid concentration, silver ion concentration and potential show how very sensitive this synthetic process can be. Fine tuning of these variables can allow for the synthesis of many different structures, optimized for many different applications.

6. Acknowledgements

The author wishes to express his appreciation to Jacilynn Brandt and Kim Rosmus from Dr. Jennifer Aitken's Research Group at Duquesne University for their assistance with XRD, SEM and EDS (supported by NSF-0511444 and NSF-0923183), Mr. Mark Donoho for his input on the electrodeposition apparatus, and Dr. Kimberly Woznick and Dr. Gregg Gould for their overall research project mentorship.

7. References

- (1) Banhart, J. *Prog. Mater. Sci.* **2001**, *46*, 559–632.
- (2) Lin, S. J. Characterization of Open Celled Metallic Foam, University of Georgia, 2010.
- (3) Shin, H.-C.; Dong, J.; Liu, M. *Adv. Mater.* **2003**, *15*, 1610–1614.
- (4) Harris, D. C. *Qualitative Chemical Analysis*; 8th ed.; W.H. Freeman and Co.: New York, 2010.
- (5) Arthur, T. S.; Bates, D. J.; Cirigliano, N.; Johnson, D. C.; Malati, P.; Mosby, J. M.; Perre, E.; Rawls, M. T.; Prieto, A. L.; Dunn, B. *MRS Bull.* **2011**, *36*, 523–531.
- (6) Finnpiette Novus Single Channel- Instructions for Use <http://fscimage.fishersci.com/images/D00174~.pdf>.